

СООБЩЕНИЯ
ОБЪЕДИНЕННОГО
ИНСТИТУТА
ЯДЕРНЫХ
ИССЛЕДОВАНИЙ

ДУБНА



C34/a

P-11

836/2-74

V.Paar

4/11/74

E4 - 7454

INTERPLAY BETWEEN
VALENCE-SHELL CLUSTERS
AND VIBRATIONAL FIELD
IN ^{94}Mo AND ^{95}Mo

1973

ЛАБОРАТОРИЯ
ТЕОРЕТИЧЕСКОЙ ФИЗИКИ

V.Paar*

INTERPLAY BETWEEN
VALENCE-SHELL CLUSTERS
AND VIBRATIONAL FIELD
IN ^{94}Mo AND ^{95}Mo

1

* Permanent address: Institute Ruđer
Bošković, Zagreb, Yugoslavia.

1. Introduction

Experimental studies of ${}^{94}_{42}\text{Mo}_{52}$ and ${}^{95}_{42}\text{Mo}_{53}$ /1-17/ reveal the coexistence between the collective and single-particle effects.

The earlier theoretical approaches to ${}^{94}\text{Mo}$ have been attempted in the framework of the shell-model calculations /18,19/, and of the collective asymmetric rotor model /17,20/, giving one-sided description of the physical situation. Specifically, shell-model calculation completely fails to predict the observed pattern of electromagnetic transitions, and the relative population of the 2^+ states in the ${}^{93}\text{Nb}({}^3\text{He}, d){}^{94}\text{Mo}$ reaction. In the shell-model calculations for ${}^{95}\text{Mo}$ /18,19/ the several observed low-lying excited states are not reproduced. Descriptions based on coupling of restricted particles or quasiparticles to vibrations, applied to ${}^{95}\text{Mo}$, face the problem of the additional effects due to the neglected neutron configurations of seniority three.

The ${}^{94}\text{Mo}$ and ${}^{95}\text{Mo}$ nuclei have two and three neutrons outside the $N=50$ closed shell, respectively, while the 28-50 proton shell is open. On the other hand, the neutron closed shell ${}^{92}\text{Mo}$ nucleus exhibits a pronounced low-frequency quadrupole mode [B(E2) ($2\ddagger \rightarrow 0\ddagger$) ~ 10 s.p.u.]. Therefore, we treat ${}^{94}\text{Mo}$ and ${}^{95}\text{Mo}$ on the same footing, by coupling valence-shell neutrons to quadrupole vibration /24-40/ and within the same parametrization. The explicit neutron configurations of seniority two and three in ${}^{94}\text{Mo}$ and ${}^{95}\text{Mo}$, respectively, turn out to be significant as was also found for few-proton clusters in ${}_{25}\text{Mn}$ /33/ ,

${}_{26}\text{Fe}$ /40/, ${}_{30}\text{Zn}$ /33/, ${}_{31}\text{Ga}$ /33/, ${}_{47}\text{Ag}$ /33/, ${}_{48}\text{Cd}$ /35,36/ ,

${}_{52}\text{Te}$ /38,39/, ${}_{53}\text{I}$ /33/, ${}_{79}\text{Au}$ /29,32,34/ and ${}_{80}\text{Hg}$ /30,36/.

In heavier Mo nuclei the particle configuration space becomes too large and one has to go to quasiparticle representation /24,26,41/. However, the explicit effect of clustering becomes less important, so a description in terms of only collective degrees of freedom can be attempted /42/.

2. The Model

In the present approach odd and even-A nuclei are treated on the same footing. The Hamiltonian is /24,25/

$$H = H_{SH} + H_{VIB} + H_{RES} + k \sum_{i=1}^n \sum_{\mu=1}^5 a_{\mu} Y_2^{\mu*}(\theta_i, \phi_i). \quad (1)$$

Here H_{SH} describes the motion of n valence-shell particles in the shell-model potential, and H_{VIB} represents the free quadrupole vibrational field. The residual interaction H_{RES} between n valence-shell particles explicitly includes only the pairing force.

The bare particle-field coupling strength is

$$a = \frac{(4\pi)^{1/2}}{3ZeR_0^2} \langle k \rangle [B^{VIB}(E_2)(2_1^+ \rightarrow 0_1^+)]^{1/2}. \quad (2)$$

The radial matrix element generally is estimated $\langle k \rangle \approx 50$ MeV /24/ and $B^{VIB}(E_2)(2_1^+ \rightarrow 0_1^+)$ has to be taken from nucleus vibrator (^{92}Mo in the case of ^{94}Mo and ^{95}Mo). The Q-Q component of the residual force, as well as high-frequency quadrupole modes and the isovector potential can be included in the renormalization of the bare particle-field coupling strength /24,43/. The effects of the isovector potential and of the bare Q-Q force act in opposite directions.

The Hamiltonian is diagonalized in the basis built from $|(j_1 j_2) J, NR; I \rangle$ and $|(j_1 j_2) J_{12}, j_3] J, NR; I \rangle$ states for $n=2$ and $n=3$, respectively. Here N and R represent the number of phonons and the angular momentum of the N -phonon state, respectively.

The E2 and M1 operators consist of a particle and a vibrational part /24,25/

$$M^\mu(E2) = \sum_{i=1}^n e^{s.p.} r_i^2 Y_2^\mu(\theta_i, \phi_i) + \frac{3}{4\pi} e^{VIB} R_0^2 (b_2^{\mu+} (-)^\mu b_2^{-\mu}), \quad (3)$$

$$\vec{M}(M1) = \left(\frac{3}{4\pi}\right)^{1/2} [g_R \vec{I} + (g_\ell - g_R) \vec{J} + (g_s - g_\rho) \vec{S}] \mu_N. \quad (4)$$

I is the total angular momentum of the nucleus, and \vec{J} and \vec{S} are the total angular momentum operator and the spin of the valence-shell cluster state, respectively. $e^{s.p.}$ and e^{VIB} are the single-particle and vibrator charge, respectively. R_0 is the nuclear radius. The quantities g_R , g_ℓ and g_s are the gyromagnetic ratios. The bare charges and gyromagnetic ratios for neutrons are $e^{s.p.} = 0$, $e^{VIB} = Z \left(\frac{\hbar\omega_2}{2C_2}\right)^{1/2}_{VIB}$, $g_R = Z/A$, $g_\ell = 0$ and $g_s = -3.82$.

3. The Calculation

In the present calculation the parametrization is chosen in a most simple-minded way directly from experiment. In this way no free parameters are present, but in interpreting results one should keep in mind possible physical renormalizations of parameters.

The neutron single-particle levels are taken as determined by the $^{92}\text{Mo}(d,p)^{93}\text{Mo}$ reaction in ref. /8/;

$$\epsilon(s_{1/2}) - \epsilon(d_{5/2}) = 1.55 \text{ MeV}, \quad \epsilon(g_{7/2}) - \epsilon(d_{5/2}) = 1.50 \text{ MeV},$$

$$\epsilon(d_{3/2}) - \epsilon(d_{5/2}) = 1.89 \text{ MeV}, \quad \epsilon(h_{11/2}) - \epsilon(d_{5/2}) = 2.22 \text{ MeV}.$$

The experimental phonon energy is taken from ^{92}Mo : $\hbar\omega_2 = 1.51$ MeV. The pairing energy is estimated in the usual way $G = 0.25$ MeV. The bare value (2) is used for the particle-vibration coupling strength: $a = 0.8$.

^{94}Mo

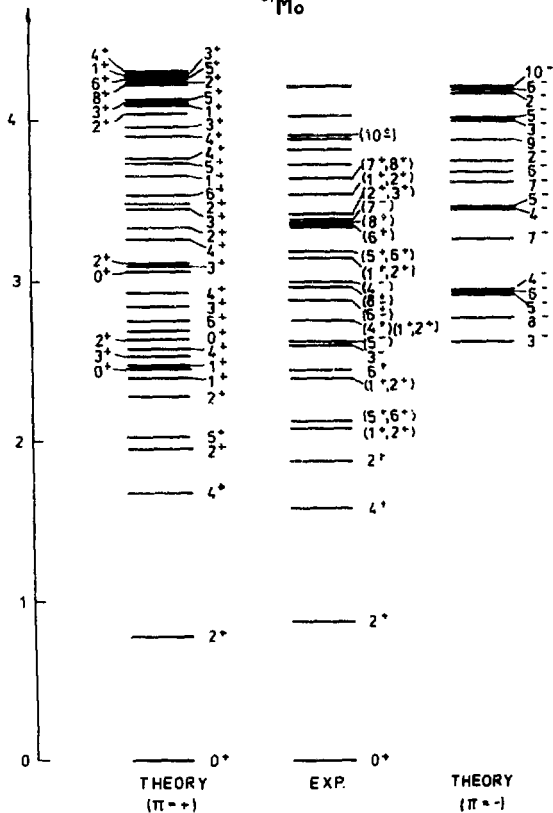


Fig. 1. Calculated and experimental levels of ^{94}Mo .

In this parametrization, without any adjustable parameter, we diagonalize Hamiltonian (1) in the corresponding basis for $n=2$ and $n=3$. The resulting calculated spectra for ^{94}Mo and ^{95}Mo are presented in figs. 1 and 2, respectively, and compared to experiment. The electromagnetic properties are obtained by calculating matrix elements of the operators (3) and (4) by using wave functions obtained by diagonalization. In tables 1 and 2 some $B(E2)$ and $B(M1)$ values are presented for ^{94}Mo and ^{95}Mo , respectively, and compared to experiment and to the calculated values of different models.

The vibrator charge $e^{VIB}=2.6$ and gyromagnetic ratios $g_R=Z/A$, $g_I=0$ have bare values, while $e^{s.p.}=0.5$ and $g_s=0.8g_s^{free}$ are renormalized in order to account for truncation and neglected velocity dependent forces, respectively /25/.

4. Static Moments

The 2_1^+ state of ^{94}Mo is in zeroth-order a one-phonon multiplet state $|(d_{5/2})^2 0, 12; 2\rangle$. The leading order contributions to the quadrupole moment come from second-order particle processes involving a single particle interacting with the electromagnetic field, and from third order induced collective processes with the absorption or emission of virtual phonons by the electromagnetic field /35,36/. The corresponding diagrams /36,37,38/ are drawn in fig. 3. To the four induced diagrams in each line, with all possible time-orderings of the phonon-electromagnetic field interaction, we apply the factorization theorem /37/. In this way, the 24 induced terms in fig. 3 can be incorporated in the "on the energy shell" effective charge

$$e_{eff}(2^+) = e^{s.p.} + \frac{5}{(\pi)^{1/2}} e^{VIB} |a| \frac{1}{h\omega_2} \quad (5)$$

which is independent of the shell-model configurations. Its effect is to enhance the shell-model effects. Therefore,

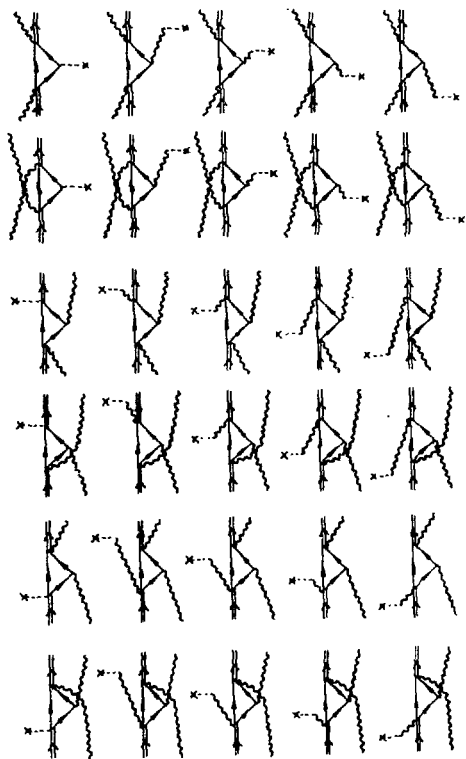


Fig. 3. Second-order particle and third-order induced collective diagrams giving leading contributions to the quadrupole moment of the first excited state.

generally the quadrupole moment is essentially the shell-effect resulting from the competition between the $Q_{CL}[(j_1 j_2) 2] > 0$ diagonal and $Q_{CL}[(j_1 j_2) 2] < 0$ nonspin-flip ($j_1 = j_2 \pm 2$ or $j_1 + j_2 = 2$) off-diagonal contribution from the valence-shell clusters. This gives a simple rule (G-VISR) for the sign and magnitude of the quadrupole moments ^{35,36/}. In ⁹⁴Mo the quadrupole moment is mainly a result of competition between the two terms: $Q_{CL}[(d_{5/2})^2] > 0$ and $Q_{CL}[(d_{5/2} s_{1/2}) 2] < 0$. For the experimental single-particle energies ^{8/}, the off-diagonal terms prevail, so the quadrupole moment is predicted to be negative ($Q = -0.27$ eb). By increasing the $s_{1/2}$ position, the off-diagonal terms become smaller and diagonal ones prevail. For $\epsilon(s_{1/2}) - \epsilon(d_{5/2}) = 5$ MeV we get $Q = 0.02$ eb. In the presence of only $d_{5/2}$ single-particle state, the off-diagonal terms are absent, and the result is $Q = 0.21$ eb.

Generally, nuclei exhibiting competition between diagonal and off-diagonal terms, are predicted to have quadrupole moments very sensitive to some single-particle positions. Classical examples of this type are Cd and ^{Te} ^{35,36/}.

The other static moments, calculated for low-lying states in ⁹⁴Mo are: $Q(4_1^+) = -0.45$ eb, $Q(2_2^+) = 0.29$ eb, $\mu(2_1^+) = 0.42 \mu_N$, $\mu(4_1^+) = 0.21 \mu_N$, $\mu(2_2^+) = -0.99 \mu_N$.

In odd nuclei the induced collective processes can also be incorporated in the effective charge (5), so the quadrupole moment is a shell-effect. The situation is greatly simplified for $N=0$ states, because in leading order there is only one contributing shell-model cluster. The corresponding contribution for the ground state of ⁹⁵Mo is $Q_{CL}[(d_{5/2})^3 5/2] = 0$, so the quadrupole moment is a higher-order, partly incoherent effect, and consequently small. This qualitative prediction is in agreement with the experimental result $Q(5/2_1^+) = \pm 0.12$ eb ^{44/}. The calculated magnetic moments of low-lying states are $\mu(5/2_1^+) = -0.55 \mu_N$ and $\mu(3/2_1^+) = -0.26 \mu_N$, and the corresponding experimental values $-0.91 \mu_N$ and $-0.39 \mu_N$ ^{44/} respectively. Magnetic moments are rather sensitive to the choice of g_κ .

5. Coexistence between Quasirotational and Quasivibrational Properties

The coexistence of quasivibrational and quasirotational characteristics is the general pattern produced by the cluster-field mechanism /30-39/.

In even nuclei, for low-lying states the quasivibrational situation is established, with strong stop-over ($0_2^+ \rightarrow 2_1^+$, $2_2^+ \rightarrow 2_1^+$, $4_1^+ \rightarrow 2_1^+$) and small cross-over ($2_2^+ \rightarrow 0_1^+$) transitions. The $2_2^+ \rightarrow 2_1^+$ E2 transition appears theoretically to be somewhat retarded with respect to the other two stop-over transitions /36/. It should be stressed, however, that the 0_2^+ , 2_2^+ and 4_1^+ model states are not based on two-phonon excitations, as supposed in the pure vibrational picture, but are of rather mixed character, involving different clusters and zero-, one-, and two-phonon components: for ^{94}Mo there are no individual components larger than 20-30%. Therefore, these states may lie rather far apart from each other, and other states can also appear in the same energy region.

The cluster-field mechanism generally reproduces the ground-state quasirotational band. The calculation for ^{94}Mo reproduces the... $10_1^+ \rightarrow 8_1^+ \rightarrow 6_1^+ \rightarrow 4_1^+ \rightarrow 2_1^+ \rightarrow 0_1^+$ band, with strong E2 transitions inside the band, and negative quadrupole moments of the members of the band, thus reflecting a kind of prolate deformation produced by the cluster-field mechanism. For higher-spin states we expect additional stretching and reduction of $B(E2)$ values (phase transition). The present model reproduces also the elements of the second band in the yrast region, but of a less pronounced quasirotational character.

For low-lying states in odd nuclei, due to cluster-field interaction, the multiplet pattern is partly broken. In ^{95}Mo the $9/2_1^+ \rightarrow 5/2_1^+$ E2 transition is strong, although both states arise from the single-particle clusters $|(d_{5/2})^3 9/2, 00; 9/2\rangle$ and $|(d_{5/2})^3 5/2, 00; 5/2\rangle$, respectively. Namely, for close-lying clusters the cluster-field interaction enhances the shell-effect, similarly as in the case of quadrupole moment /36/. The $7/2_1^+ \rightarrow 5/2_1^+$ E2 transition is forbidden due to spin-flip selection rule

($7/2_1^+$ state is based on the $[(d_{5/2})^0, g_{7/2}] 7/2, 00; 7/2$ configuration), and therefore retarded. The $1/2_1^+ \rightarrow 5/2_1^+$, $3/2_1^+ \rightarrow 5/2_1^+$ and $7/2_2^+ \rightarrow 5/2_1^+$ transitions are strong because they are of $\Delta N=1$ type, and there is no lower-lying nonspin-flip cluster state of the same spin as initial state /33,36/.

Typical quasirotational elements in odd nuclei, produced by the cluster-field mechanism, are the quasirotational band and the $l=j-1$ anomaly. The general result are the strong $\Delta l=2$ E2 transitions inside the two sequences ... $21/2_1^+ \rightarrow 17/2_1^+ \rightarrow 13/2_1^+ \rightarrow 9/2_1^+ \rightarrow 5/2_1^+$ and ... $23/2_1^+ \rightarrow 19/2_1^+ \rightarrow 15/2_1^+ \rightarrow 11/2_1^+ \rightarrow 7/2_2^+ \rightarrow 5/2_1^+$ of the ground state band. This feature is based on the mechanism of maximum alignment, which is the geometrical effect as in the deformed region. The calculated quadrupole moments of the numbers of the ground-state band are negative, as for the neighbouring even ^{94}Mo . For higher spins additional effects due to appearance of phase transition are also expected.

The $l=j-1$ anomaly, i.e. the lowering of the one-phonon multiplet state $[(d_{5/2})^3 5/2, 12; 3/2 >$ relatively to the other states of the multiplet is an explicit effect of Pauli principle between the three valence-shell neutrons, enhanced due to mechanism of the cluster-field coupling /33/. The pronounced collective character of the $3/2_1^+$ state is reflected in strong $3/2_1^+ \rightarrow 5/2_1^+$ E2 transition. For higher spins and stronger coupling the state is more lowered and decreases even below the cluster state $j(^{51,55}\text{Mn}, ^{107,109,111}\text{Ag}, \text{etc.})$ /33/.

6. Transfer Properties

Transfer-reactions involving ^{94}Mo , ^{95}Mo and neighbouring nuclei /6-11/ reveal appreciable single-particle clustering, i.e. deviations from a simple vibrational picture.

The $5/2^+$ ground state of ^{93}Mo is strongly and the higher states weakly excited in the $^{94}\text{Mo}(d,t)^{93}\text{Mo}$ transfer

reaction /6/. The ground states of ^{93}Mo and ^{94}Mo are based on the $|d_{5/2}, 00; 5/2\rangle$ and $|(d_{5/2})^2 0, 00; 0\rangle$ zeroth-order configurations, respectively. The ground state of ^{93}Mo is therefore populated by zeroth order processes in both (d,t) and (d,p) reactions. The states based on other single-particle states, namely $1/2_1^+$, $3/2_1^+$ and $7/2_1^+$ are populated by first order pairing processes in the (d,t) reactions, whereas in the (d,p) reaction they are directly excited. The states based on single-particle multiplets are populated by higher-order processes.

In the $^{94}\text{Mo}(p,t)^{92}\text{Mo}$ reaction the ground state of ^{92}Mo is rather strongly excited, and the other low-lying states are weakly populated /9/. The $(d_{5/2})^2 0, (s_{1/2})^2 0$, $(g_{7/2})^2 0$, $(d_{3/2})^2 0$ and $(h_{11/2})^2 0$ neutron pairs in the ground state wave function contribute coherently to the form factor for the $0_1^+ \rightarrow 0_1^+$ two-particle transfer. The ratio of the $(s_{1/2})^2 0$ to the $(d_{5/2})^2 0$ strength obtained in our calculation is 0.1. The $0_1^+ \rightarrow 2_1^+$ (p,t) transfer in the present model follows mainly from one-phonon components in the ground state of ^{94}Mo with the $(d_{5/2})^2 2$, $(d_{5/2} s_{1/2})^2$ and $(s_{1/2} d_{3/2})^2$ broken neutron pairs.

The $^{93}\text{Nb}(^3\text{He},d)^{94}\text{Mo}$ reaction yields a pronounced experimental result: the lowest 2_1^+ state is more strongly excited than the second 2_2^+ state by one order of magnitude /10/, which contradicts to the shell-model calculations /18, 19/. The present approach naturally accounts for the experimental situation. The ^{93}Nb ground state in zeroth order arises from a $g_{9/2}$ quasiproton coupled to a $(d_{5/2})^2 0$ neutron pair. In this way the $^{93}\text{Nb}(^3\text{He},d)^{94}\text{Mo}$ reaction mainly excites the $|(d_{5/2})^2 0, 12; 2\rangle$ component through the $(g_{9/2})^2 2$ two-quasiproton configurations, creating a phonon by a first-order process. The 2_1^+ and 2_2^+ states in ^{94}Mo arise from the $|(d_{5/2})^2 0, 12; 2\rangle$ and $|(d_{5/2})^2 2, 12; 2\rangle$ basic configurations, respectively. Therefore, the basic component of the 2_1^+ state is populated by the first-order and that of the 2_2^+ state by the third-order process, being an order of magnitude smaller.

The $^{95}\text{Mo}(d,t)^{94}\text{Mo}$ and $^{94}\text{Mo}(p,p'\gamma)$ reactions reveal appreciable excitation of the 0_1^+ , 2_1^+ and 4_1^+ states, the 4_1^+ state being more strongly excited than the

2_1^+ state /11/. In the present approach the 0_1^+ and 4_1^+ are based on $|(d_{5/2})^{20,00;0}\rangle$ and $|(d_{5/2})^{24,00;4}\rangle$ zero-phonon components, respectively, while the 2_1^+ state is based on the $|(d_{5/2})^{20,12;2}\rangle$ one-phonon component. The ground state of ^{95}Mo arises from the $|(d_{5/2})^{35/2,00;5/2}\rangle$ component. Therefore, in zeroth order $5/2_1^+ \rightarrow 0_1^+$ and $5/2_1^+ \rightarrow 4_1^+$ transfer is allowed and $5/2_1^+ \rightarrow 2_1^+$ forbidden. Pairing correlations increase the population of the 0_1^+ state, and first-order particle-vibration coupling processes contribute to the excitation strength of the 2_1^+ state.

In the $^{94}\text{Mo}(d,p)^{95}\text{Mo}$ reaction the experimental spectroscopic factors of the low-lying states are $5/2_1^+(0.59)$, $3/2_1^+(0.02)$, $7/2_1^+(0.18)$ and $1/2_1^+(0.37)$ ^{16/}. The corresponding direct components (populating $|(d_{5/2})^{20,00;0}\rangle$ configuration in ^{94}Mo) in our wave functions for ^{95}Mo give 0.56, 0.03, 0.36 and 0.40, respectively. It should be stressed that (d,p) experiment clearly shows that the $3/2_1^+$ state is not of one-particle or one-quasiparticle character, i.e. that its origin lies in $l=j-1$ anomaly, which is due to neutron cluster of seniority three.

7. Conclusion

Shell-model calculations could, in principle, give the proper description of so-called spherical and transitional nuclei, provided the full space of all active configurations contributing noticeably to the properties of the nuclear system is taken into account. However, one is forced to truncate the space rather severely, which leads to a loss in amount of physical information.

Alternative approaches are based on describing the nuclear system in terms of only collective variables obtained by averaging over the shell-model structure. Such approaches are applied, when the averaging is expected to be a fair representation of the actual situation, and no explicit shell-model configurations are important.

Explicit shell effects could then be included by coupling dominant valence-shell few-particle clusters to the col-

lective field. In this way much larger effective space is included than in the corresponding shell-model calculations. The two simple choices of the basic representations are:

i) Spherical representation, i.e. coupling of single particles in shell-model spherical configurations to vibrations.

ii) *Deformed representation*, i.e. coupling of single particles in Nilsson orbitals to rotations.

Both representations can be used to describe an intermediate physical situation in spherical and transitional nuclei, which is characterized by the coexistence of the quasirotational, quasivibrational and clustering patterns. The cluster-field interaction and Pauli principle introduce quasirotational elements into (i), while the Coriolis coupling introduces quasivibrational elements into (ii).

In the present paper we have demonstrated the approach (i) on ^{94}Mo and ^{95}Mo . However, in the light of simple-minded parametrization and of the neglected correlations, the quantitative results should not be interpreted too rigidly.

Possible generalizations can be attempted in two directions: a) including additional types of correlations, b) extension to larger clusters. In the case b) transition to the BCS basis seems to be appealing. However, the present approaches to $n=2$ and $n=3$ systems indicate the importance of higher-seniority configurations.

Acknowledgement

The author expresses his gratitude to Professor G. Alaga for valuable discussions and continuous support and thanks the Joint Institute for Nuclear Research for the stay in Dubna, during which the work was finished.

References

1. Yu.P.Gangrskii and I.Kh.Lemberg. *Izv.Akad. Nauk SSSR (ser. fiz)*, 26, 1001 (1962).
2. S.Monaro, G.B.Vingiani, R.A.Ricci, R. Van Lieshout. *Physica*, 28, 63 (1962).
3. N.K.Aras, E.Eichler, G.G.Chilosi. *Nucl.Phys.*, A112, 609 (1968).
4. J.M.Jaklevic, C.M.Lederer, J.M.Hollander. *Nucl.Phys.*, A169, 449 (1971).
5. J.Barette, M.Barette, A.Boutard, R.Haroutunian, G.Lamoureux, S.Monaro. *Phys.Rev.*, C6, 1339 (1972).
6. R.C.Diehl, B.L.Cohen, R.A.Moyer, L.H.Goldman. *Phys.Rev.*, C1, 2132 (1970).
7. S.A.Hjorth, B.L.Cohen. *Phys.Rev.*, 135B, 920 (1964).
8. J.B.Moorhead, R.A.Moyer. *Phys.Rev.*, 184, 1205 (1969).
9. A.Moalem, M.A.Moinester, N.Auerbach, J.Alster, Y.Dupont. *Nucl.Phys.*, A177, 145 (1971).
10. M.R.Cates, J.B.Ball, E.Newman. *Phys.Rev.*, 187, 1682 (1969).
11. E.Abramson, G.Engler, Z.Vager, N.Cue, J.Plessner, G.F.Wheeler. *Phys.Lett.*, 38B, 70 (1972).
12. F.K.McGowan, P.H.Stelson. *Phys.Rev.*, 109, 901 (1958).
13. J.Barette. Private communication.
14. P.D.Bond, S.Jha. *Phys.Rev.*, C2, 1887 (1970).
15. D.G.Alkhazov, K.I.Ekokhina, I.Kh.Lemberg. *Izv. Akad. Nauk. SSSR (ser. fiz.)*, 28, 1667 (1964).
16. L.Mesko, A.Nilsson, S.A.Hjorth, M.Brenner, O.Holmlund. *Nucl.Phys.*, A181, 566 (1972).
17. J.Barette, A.Bouratd, S.Monaro. *Can.J.Phys.*, 47, 995 (1969).
18. J.Vervier. *Nucl.Phys.*, 75, 17 (1966).
19. K.H.Bhatt, J.B.Ball. *Nucl.Phys.*, 63, 286 (1965).
20. A.S.Davidov, A.A.Chaban. *Nucl.Phys.*, 20, 499 (1960).
21. D.C.Choudhury, J.T.Clemens. *Nucl.Phys.*, A125, 140 (1969).
22. B.S.Reehal, R.A.Sorensen. *Phys.Rev.*, C2, 819 (1970).
23. L.Kisslinger, K.Kumar. *Phys.Rev.Lett.*, 19, 1239 (1969).
24. A.Bohr, B.R.Mottelson. *Mat.Fys. Medd. Dan. Vid. Selsk.*, 27, No. 16 (1953); *Nuclear Structure*, vol.2, to be published.
25. G.Alaga. *Rendconti Scuola Internazionale di Fisica "E.Fermi"*, Varenna, XL Corso, 28, 1967 and references quoted therein.
26. V.G.Soloviev. *Theorija slozhnykh jader*, Izd-vo "Nauka", Moskva, 1971.
27. D.C.Choudhury. *Mat. Fys. Dan. Vid. Selsk.*, 28, No. 4 (1954).

28. B.J.Raz. Phys.Rev., 114, 1116 (1959).
29. G.Alaga. Bull. Am. Phys.Soc., 4, 359 (1959).
30. G.Alaga, G.Ialogne. Phys.Lett., 22, 619 (1966).
31. G.Alaga, F.Krmpotic, V.Lopac. Phys.Lett., 24B, 537 (1967).
32. G.Alaga, G.Ialongo. Nucl.Phys., A97, 600 (1967).
33. V.Paar. Phys.Lett., 39B, 466 (1972); 39B, 587 (1972); 42B, 8 (1972) and Nucl.Phys., to be published.
34. G.Alaga, V.Paar, to be published.
35. G.Alaga, V.Paar, V.Lopac. Phys.Lett., 43B, 459(1973).
36. G.Alaga, F.Krmpotić, V.Lopac, V.Paar, L.Sips., to be published.
37. V.Paar. Nucl.Phys., A164, 576 (1971); A164, 593 (1971); A166, 341 (1971); Proceedings XV International Summer Meeting on Nuclear Structure, Herceg Novi, Yugoslavia 1970, Edited by A.H.Kukoc, Belgrade; and to be published.
38. V.Lopac. Thesis, University of Zagreb, 1971.
39. V.Lopac. Nucl.Phys., A155, 513 (1970).
40. V.Paar. Nucl.Phys., A185, 544 (1972).
41. A.I.Vdovin, Ch.Stojanov. JINR, P4-6912, Dubna, 1973.
42. R.Jolos, F.Donau, D.Janssen.JINR, P4-7144, Dubna, 1973.
43. R.A.Brogia, V.Paar, D.R.Bes. Phys.Lett., 37B, 159, 257 (1971).
44. Nuclear Data Sheets.

Received by Publishing Department
on September 12, 1973.

Table 1
 Comparison of available experimental and theoretical
 B(E2) and B(M1) values for ^{94}Mo

	EXPERIMENT	THEORY	
		VERVIER ^c	PRESENT
$B(E2)(2_1^+ \rightarrow 0_1^+)$	0.054 ± 0.008^a 0.044 ± 0.002^b	0.037	0.050
$B(E2)(2_2^+ \rightarrow 0_1^+)$	0.0011 ± 0.0003^a 0.0006 ± 0.0001^b	0.046	0.001
$B(E2)(2_1^+ \rightarrow 2_1^+)$	0.031^a 0.116 ± 0.026^b	0.035	0.033
$B(E2)(4_1^+ \rightarrow 2_1^+)$	0.067 ± 0.010^b		0.057
$B(M1)(2_1^+ \rightarrow 2_1^+)$	0.020 ± 0.007^b	3.76	0.021

^aRef./1/

^bRef./5/,

^cRef./18/

Table 2
Comparison of available experimental and theoretical
B(E2) and B(M1) values for ^{95}Mo

	EXPERIMENT	THEORY			
		CHOUDHURY CLEMENS ^f	REEHAL SORENSEN ^g	KISSLINGER KUMAR ^h	PRESENT
B(E2)($3/2_1^+ \rightarrow 5/2_1^+$)	0.053 \pm 0.005 ^a 0.059 \pm 0.004 ^b 0.064 \pm 0.007 ^c	0.057	0.024	0.015	0.052
B(E2)($7/2_1^+ \rightarrow 5/2_1^+$)	0.005 \pm 0.003 ^d <0.0003 ^b \leq 0.0005 ^c	0.042	0.012	0.007	0.005
B(E2)($1/2_1^+ \rightarrow 5/2_1^+$)	0.060 \pm 0.015 ^f 0.009 \pm 0.001 ^j	0.045	0.121	0.042	0.021
B(E2)($(3/2_2^+, 5/2_2^+) \rightarrow 5/2_1^+$)	0.0006 \pm 0.0002 ^b				0.000
B(E2)($3/2_1^+ \rightarrow 5/2_1^+$)	0.019 \pm 0.005 ^e 0.032 \pm 0.003 ^b 0.030 \pm 0.003 ^c				0.026
B(E2)($1/2_2^+ \rightarrow 5/2_1^+$)	0.015 \pm 0.003 ^b				0.004

Table 2 (cont.)

$B(F_2)(3A_1^+ \rightarrow 5A_1^+)$	0.011 ± 0.002^b				0.006
$B(M_2)(7/2_2^+ \rightarrow 5/2_2^+)$	0.022 ± 0.005^c				0.017
	0.029 ± 0.003^b				
	0.030 ± 0.004^c				
$B(M_1)(3/2_1^+ \rightarrow 5/2_1^+)$	0.0044^a				0.033
	0.0045 ± 0.0008^b				

^aRef./12/, ^bRef./13/, ^cRef./44/, ^dRef./14/, ^eRef./15/, ^fRef./21/, ^gRef./22/, ^hRef./23/